

UNIVERSAL VELOCITY AND TEMPERATURE DISTRIBUTIONS IN FORCED CONVECTION THROUGH SQUARE DUCT WITH ASYMMETRIC HEATING

Khan Rezaul Karim¹, Md. Morad Hossain Mollah², M. A.T. Ali³, M. A. R. Akhanda⁴
and Md. A. R. Sarkar⁵

^{1,2}Department of Mechanical Engineering, Bangladesh University of Engineering and Technology, Dhaka,
^{3,4,5}Professor, Department of Mechanical Engineering, Bangladesh University of Engineering and Technology,
Dhaka

ABSTRACT

The velocity and temperature at a number of layers of Z-axis starting from the nearest point of the bottom-heated surface and perpendicular to the Y-axis have been measured for turbulent air flow through a non-ribbed square duct with asymmetric heating. Velocity and temperature have also been measured at a number of layers of Y-axis starting from the nearest point of side-wall and perpendicular to the Z-axis. Universal velocity and temperature have been calculated from these measured values. Moderate heat transfer rate has been employed at Reynolds number of $Re=5.0 \times 10^4$ and $Re=5.6 \times 10^4$. Universal velocity and temperature distributions have been evaluated at three different sections of the test duct of $X/D_h=3$ and 33. A number of empirical correlations related to the velocity and temperature inner laws have been developed which correlate all data generated in the experiments and finally the results have been compared with other relations available in the literature

Keywords: Hat Shaped, Saddle Shaped, Strong Secondary flow, Friction Factor and. Ribbed wall.

1. INTRODUCTION

In narrow channel the boundary layer formation on the side walls interferes with the boundary layer growth at the bed of the channel. Consequently, in the corners the loss of energy is more than that in the rest of the cross-section. A mass-transport mechanism operates to maintain flow in the corners. The cross-flow pattern thus set up to supply more fluid at the corners from the rest of the cross-section is called the secondary flow pattern. These types of secondary flows are always set up in the straight channels. In general, the secondary flow are set up by virtue of the transverse pressure gradients set up in the main flow and thus retards the flow velocity.

Secondary flow of Prandtl's second kind¹ is one of the most characteristics phenomena observed in turbulent flows through non-circular ducts.²⁻³ Although velocities of the secondary flow amount to at most several percent of the maximum primary velocity. Myong⁴ found in his investigation that the magnitude of the turbulence-driven secondary motion is only of the order of 2-3 percent of the stream wise mean velocity. The secondary flow has a great influence on flow and temperature field⁵⁻⁷. The behaviour and the origin of the secondary flow of the second kind have attracted the interest of many investigators and numerous studies have been reported in connection with the flow, specially with that in smooth-walled square duct.⁸⁻¹³

Forced convection heat transfer in entrance region of

non-circular ducts. So far as it is known, none have conducted experiments for turbulent forced convection heat transfer in entrance region of a non-circular duct. For this reason, researchers of present study are interested to investigate the heat transfer characteristics for turbulent flow through the developed region of ribbed and non-ribbed square duct.

2. EXPERIMENTAL SETUP

An experimental set-up has been designed to investigate the universal velocity and temperature in developing flow through a square duct. At room temperature and atmospheric pressure air is introduced into the square duct through a contraction. The overall length of the test duct is 5755mm, which are divided into three parts. They are the hydrodynamic developing duct of length 3000mm, the developed duct of length 1830mm and the rear duct of length 925mm. The hydraulic diameter of the duct is 50mm. Bakelite sheet of 16mm thick is used to make its side walls. The top wall is made of 12.5mm thick clear perspex sheet and is fastened with the side walls by means of Allen bolts. The bottom (non-ribbed) wall of the duct is made of 12.5mm thick aluminium wall. A flexible duct (damper) is placed at the outlet of the rear duct. A diffuser of length 920mm is introduced between the outlet of the flexible duct and the inlet of the fan motor having 2.75 hp and 2900 rpm. A silencer is mounted at the outlet of the fan motor to

minimize creating sound and vibration. A butter-fly is set-up at the other end of the silencer to control the flow rate of air for measuring the required Reynolds number.

3. WORKING PROCEDURES OF THE EXPERIMENTS

At the beginning of every set of experiment, a specified target temperature is fixed to the temperature controller. The voltage and current supplied to the heater are recorded from a digital voltmeter and a digital ammeter and thus heat energy generated to the heater is calculated. Eleven thermocouples are positioned to the bottom surface of the aluminium wall to measure its temperatures. The distributions of thermocouples are at a distance of 163mm, along the bisector of the bottom surface and a digital thermocouple thermometer with a selector switch is used to record the temperatures at their respective positions. The mean temperature of the bottom surface is calculated by averaging the recorded temperatures and the mean temperature of its inner surface is evaluated using corrected equation.

The temperatures and velocities of the heated air flowing in the test duct are measured for 494 In Y-Y axis and 507 in Z-Z axis specified points across its inlet and outlet. From the recorded data the average temperature and average velocity at inlet and outlet are calculated for every set of experiment. Thus, the mean temperature and mean velocity of flow are evaluated by averaging those average temperatures and average velocities. For each set of experiment, static pressures at wall are measured from six pressure-taps.

4. EQUATIONS, UNITS AND NOMENCLATURE

(i) Effect of Reynolds Number on Mean Temperature of Air Flowing in the Test Ducts

Figure 1-2 shows the effect of Reynolds numbers on mean temperature of air flowing through a non-ribbed and twelve-ribbed ducts. From these figures it is observed that any ribbed duct shows higher mean temperature over the non-ribbed duct. The ribbed wall increases the total surface area of the bottom heated wall which enhances convection heat transfer from the inner surface to the air flowing in the duct. The rib breaks the laminar sub-layer and creates local wall turbulence along with flow separation, reversal of flow and reattachment between the adjacent ribs and these help to exchange more amount of heat to the flowing air in the duct. So, the mean temperature of air flowing in the duct with ribbed wall is higher than that of the duct having non-ribbed wall. The effect of Reynolds numbers on mean temperature of air and their percentage of increase have been evaluated. The percentage increasing of mean temperature for seven Reynolds numbers are calculated on the basis of the result obtained for non-ribbed wall at $Re = 5.6 \times 10^4$. The mean temperature of air flowing in the test duct at this Reynolds number is considered to be 100 percent and the other results have been compared with it. It is observed that the percentage increase of mean temperature of air for ribbed wall having higher values for all the corresponding Reynolds number over the non-ribbed wall. For different Reynolds number the

duct with ribbed wall of $p/e = 8$ shows the percentage increase of mean temperature of different magnitude for different rib shape. From the analysis, it may be concluded that the lower Reynolds number yields the higher percentage of mean temperature of flowing air over that at the higher Reynolds number.

The effect of rib pitch to height ratios (p/e) on mean temperature of air flowing in different ribbed ducts at seven Reynolds numbers is shown in Figs. 3-4. It is shown that mean temperature of air for each Reynolds number decreases gradually with an increasing value of p/e . The figure also shows that the duct with ribbed wall having shorter rib pitch to height ratio (p/e) shows the higher value than that of the longer on. This is because of the reason explained earlier. It is found that at $Re = 5.6 \times 10^4$ the mean temperature of air flowing through twelve ribbed ducts of $p/e = 10, 8$ and 6 increasing about 100.54, 100.65 and 100.71 percent in triangular ribs, 100.59, 100.70 and 100.76 percent in saw tooth forward ribs, 32.43, 100.53 and 100.64 percent in backward ribs, 100.48, 100.58 and 100.65 percent in trapezoidal ribs respectively over the non-ribbed duct.

Eventually, it may be concluded that higher Reynolds number have the lower percentage increase of mean temperature of air flowing through the ducts. Whereas, they have the higher values in the lower p/e ratio ducts.

(ii) Mean Flow Velocity Distributions along the Z-axis in Ribbed Ducts

Figures 5-6 show the mean flow velocity distributions across Z-axis at $X/D = 3$ and 33 and $Re = 5.0 \times 10^4$ and 5.6×10^4 respectively for triangular ribbed-roughened ducts with $p/e = 6$.

The nature of velocity profiles of the ribbed duct is found to be invariant with the change of Reynolds number from 5.0×10^4 to 5.6×10^4 as found in non-ribbed duct; the profiles also behave symmetrically along the Z-axis. Unlike non-ribbed duct the profiles of the ribbed roughened duct show hat-shape velocity profile. This hat shape is between the parabolic shape and saddle shape profile indicating the presence of weak secondary velocity.

(iii) Mean Temperature Distributions along Z-axis in Square Non-Ribbed and Ribbed Ducts

Figure 7-8 show the temperature distributions at $X/D = 33$. The investigations have been carried out at seven different levels of $Y/B = 0.00, -0.2, -0.4, -0.6, -0.7, -0.8$ and -0.9 in the Y-Z plane at $Re = 5.0 \times 10^4$ and 5.6×10^4 respectively. Temperatures are measured at 39 different points for every level as shown in Fig. 4.3f. In the figures fluid temperature (T) is subtracted from the average temperature of the inner surface of the heated wall (T_{wi}) and the result is divided by the temperature difference of T_{wi} and T_{co} , the centreline fluid temperature. Thus the dimensionless temperature parameter $(T - T_{wi}) / (T_{wi} - T_{co})$ is taken as the indicating temperature of the flow field. In the figures all the temperature profiles show its minimum value at the centre of the duct along the Z-axis ($Z/B = 0$). The profiles clearly indicate the systematic decrease of fluid temperature with the increase of wall distance. The profiles along the z-axis can distinctly be divided into three zones viz wall zone, $(-1.0 > Z/B < -0.4)$,

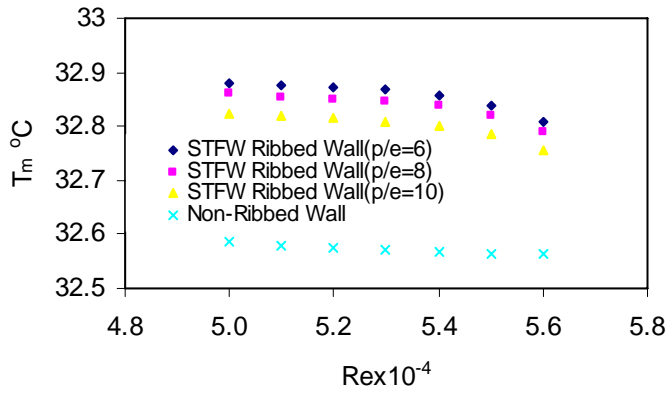


Fig 1: Effect of Reynolds number on mean temperature of air in saw tooth Forward ribbed ducts

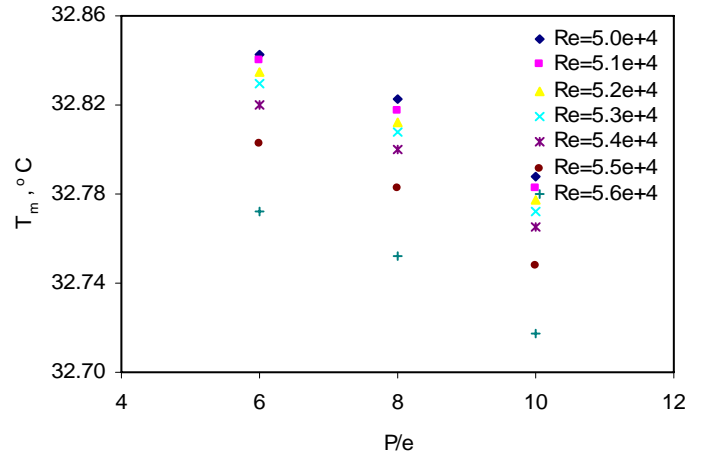


Fig 4: Effect of Rib Pitch to height ratio on mean temperature of air in Trapezoidal ribbed ducts

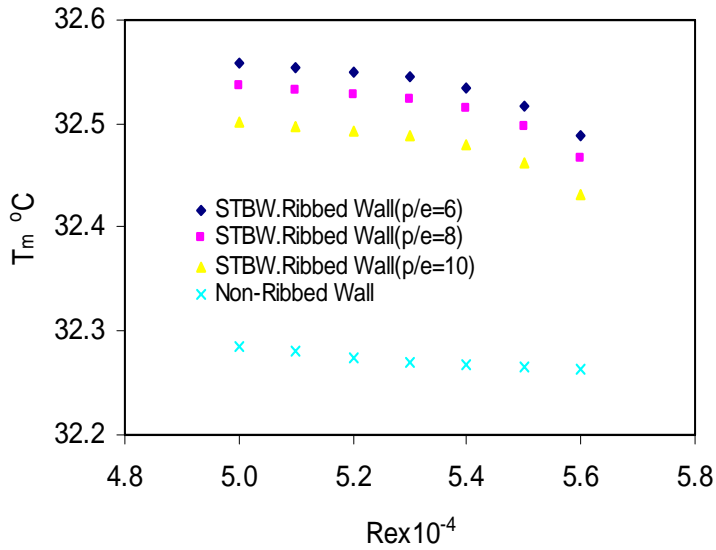


Fig 2: Effect of Reynolds number on mean temperature of air in saw tooth Backward ribbed ducts

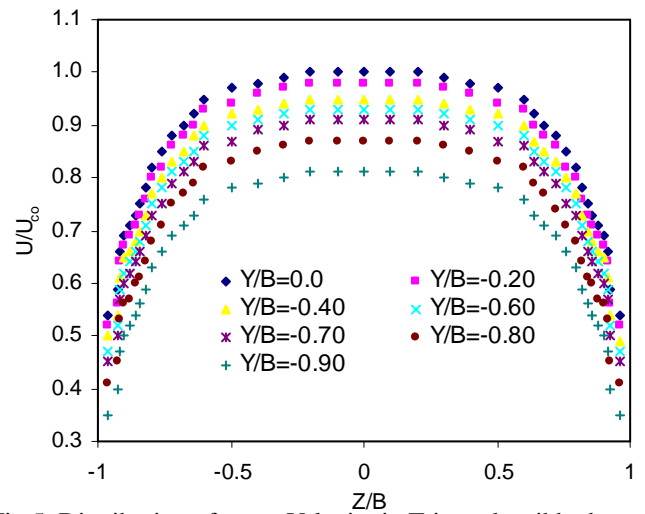


Fig 5: Distribution of mean Velocity in Triangular ribbed duct (p/e=6) at X/D=3 (Re = 5.0x10⁴)

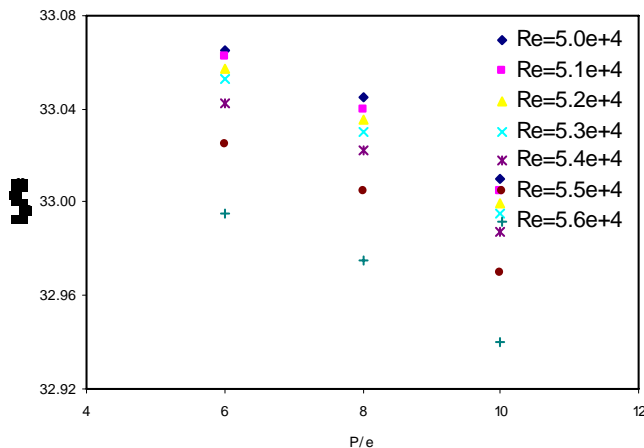


Fig. 3 Effect Of Rib Pitch to Height Ratio on Mean Temperature of air in triangular Ribbed Ducts.

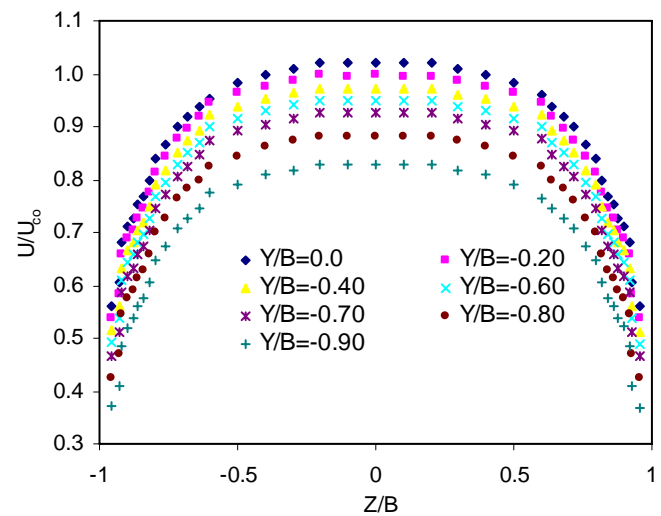


Fig 6: Distribution of mean Velocity in Triangular ribbed duct (p/e=6) at X/D=33 (Re = 5.0x10⁴)

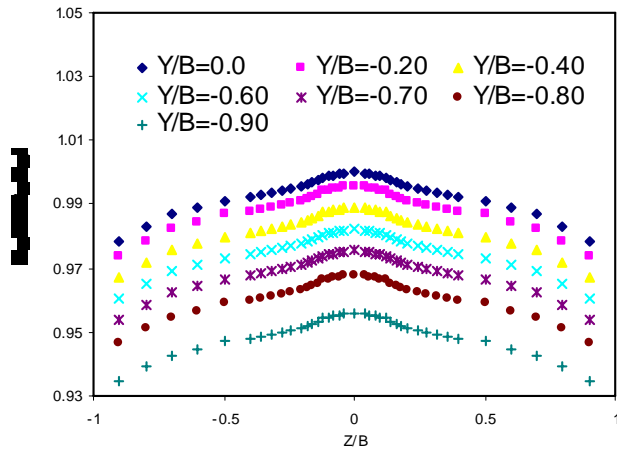


Fig 7: Temperature distribution in Ribbed duct along Z axis at $X/D_h=33$ (STFW, $p/e=8$, $Re=5.0 \times 10^4$)

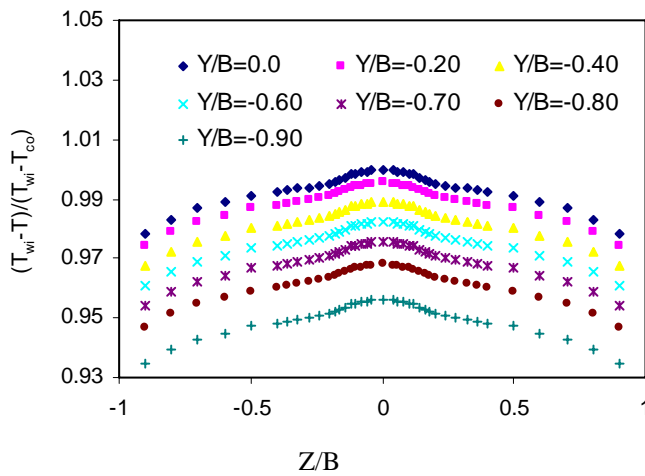


Fig 8: Temperature distribution in Ribbed duct along Z axis at $X/D_h=33$ (Tri, $p/e=8$, $Re=5.0 \times 10^4$)

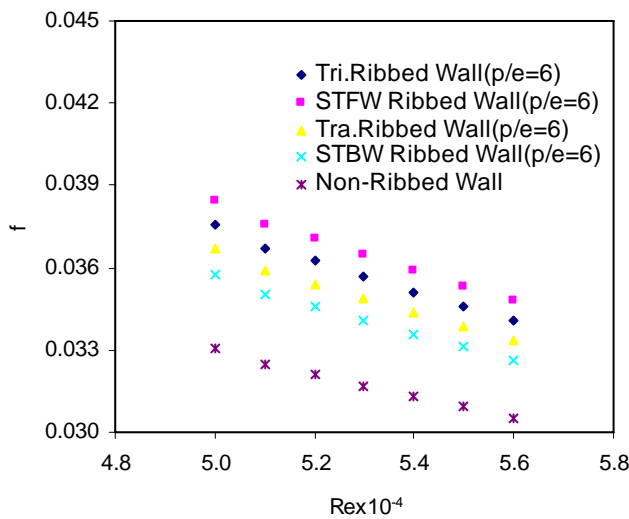


Fig 9 Effect of Reynolds Number on Friction Factor for various types of Ribbed walls.

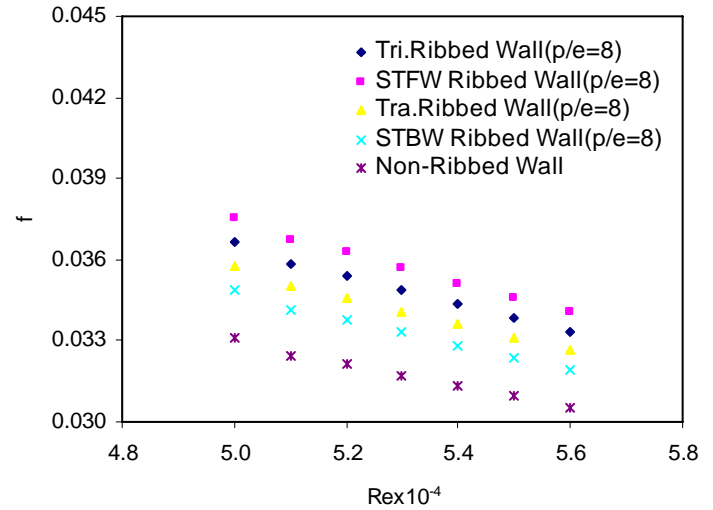


Fig 10 Effect of Reynolds Number on Friction Factor for various types of Ribbed walls.

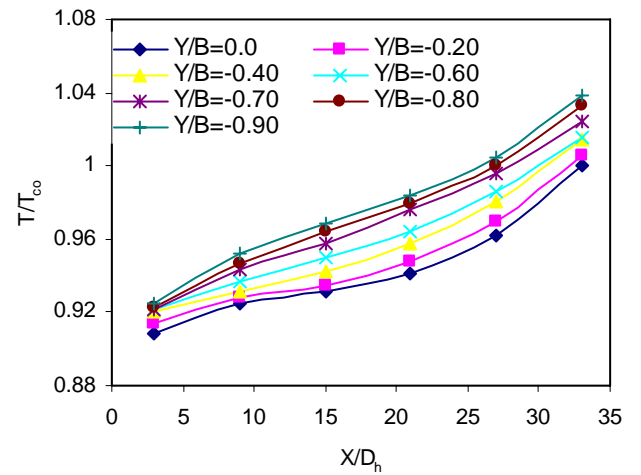


Fig.11 Temperature Distributions along X-Axis at different wall distance (Y/B) for Triangular Ribbed Wall at $p/e=6$ ($Re=5.2 \times 10^4$).

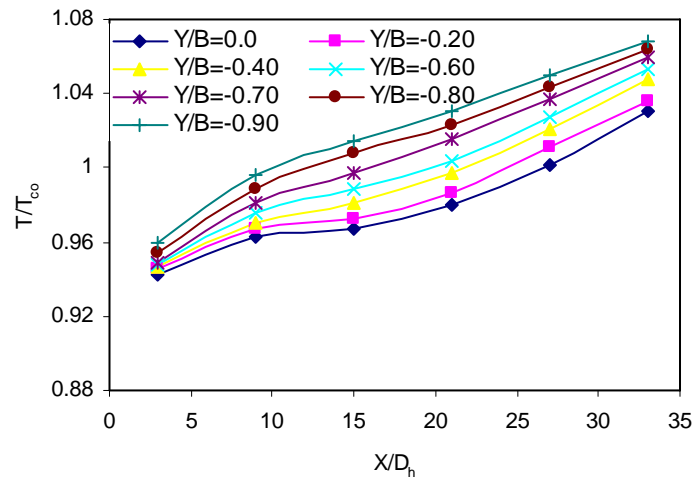


Fig..12 Temperature Distributions along X-Axis at different wall distance (Y/B) for Trapezoidal Ribbed Wall at $p/e=10$ ($Re=5.2 \times 10^4$)

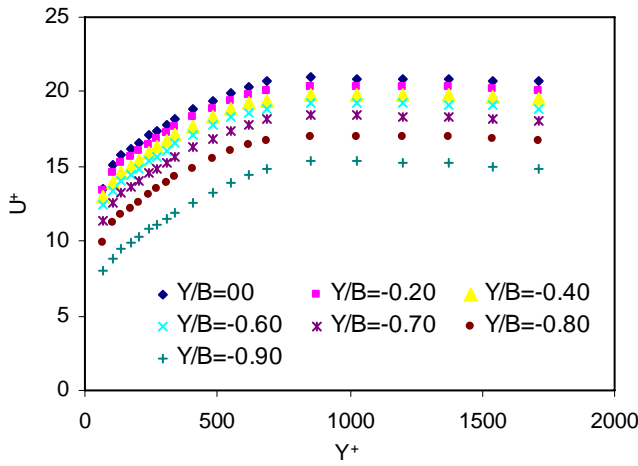


Fig. 13 Universal Velocity Distributions for Non-Ribbed Duct at $X/D_h=33$ from $Z/B=0.90$ to 0.0 ($Re=5.0 \times 10^4$)

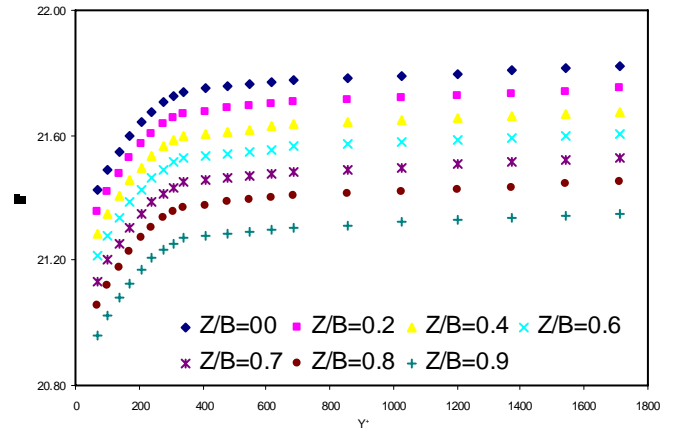


Fig. 14 Temperature Distributions parallel to the heated wall in Non-Ribbed Duct at $X/D_h=33$ from $Y/B=-0.90$ to 0.0 ($Re=5.0 \times 10^4$)

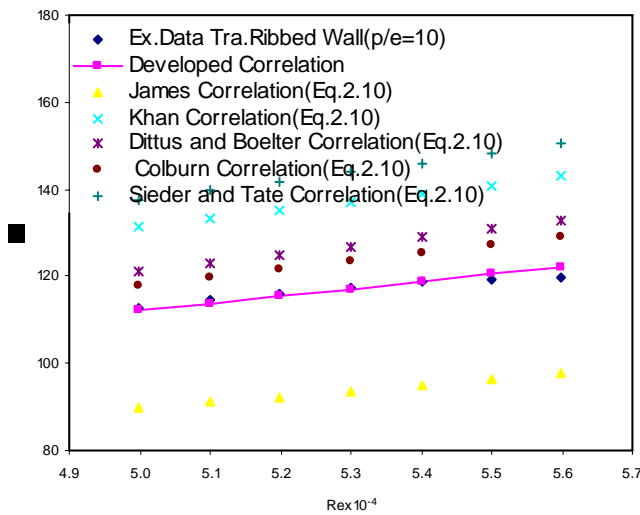


Fig. 15 Developed Correlation for Ribbed Ducts in Hydrodynamically Developed Region

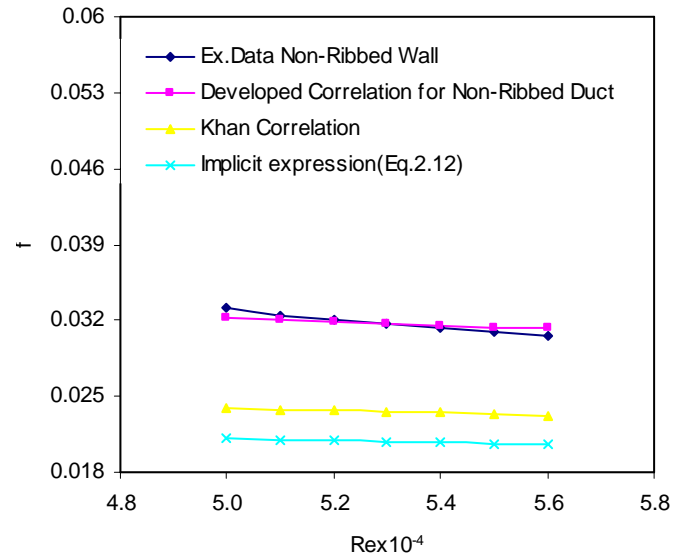


Fig. 16: Developed correlation for ribbed ducts

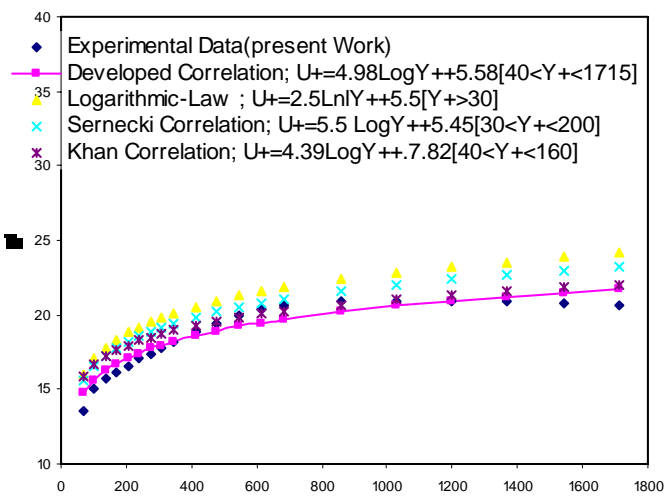


Fig. 17 Developed Correlations of Universal Velocity Distribution in Non-Ribbed Duct With Others Equation ($Y/B=0.0, -0.90 < Y/B < 0.0, Re=5.0 \times 10^4$)

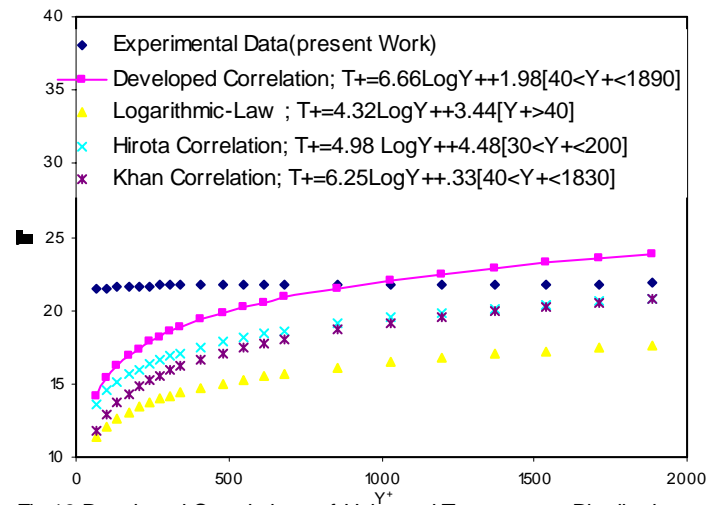


Fig. 18 Developed Correlations of Universal Temperature Distribution in Non-Ribbed Duct With Others Equation ($Z/B=0.0, -0.90 < Y/B < 0.05, W, Re=5.6 \times 10^4$)

mid plane zone ($-0.4 > Z/B < -0.8$) and central zone ($-0.8 > Z/B < 0$). In the wall zone the effect of boundary layer is prominent on the temperature profile. In this zone temperature is found to decrease nearly with the wall distance. In the mid plane zone the effect of secondary flow is prominent. In this zone secondary flow carries high temperature fluid from near the wall towards this zone creating a nearly constant air temperature zone in this region. In the central zone the presence of weak secondary flow weakens the air mixing process thereby carrying less heat to this zone from near the heated wall region. Due to this fact the temperature in this zone decreases sharply creating the minimum temperature at the centre ($Z/B = 0$).

(iv) Effect of Reynolds number on Friction Factor for Various Types of Ribbed Walls

The variation of friction factor with Reynolds number is shown in figures 9 to 10. All the figures show the decrease of friction factor nearly linearly with the increase of Reynolds number. The friction factor curves for STFW, Triangular, Trapezoidal, Saw Tooth Backward and smooth ducts as shown in figure 9 can be expressed as

$$f_{STFW} = -0.006 Re + 0.0681$$

$$f_{Tri} = -0.0057 Re + 0.0657$$

$$f_{Tra} = -0.0054 Re + 0.0633$$

$$f_{STBW} = -0.005 + 0.0609$$

$$f_{max} = -0.0041 Re + 0.0537 \text{ respectively}$$

(v) Development of Correlations:

Figures 15-18 shows the curve fitting to the data obtained from the experiments of the ducts having ribbed and smooth walls. The curve fittings have developed two correlations, which are used for the determination of forced convection heat transfer in the similar types ducts with ribbed wall and smooth wall as given in the following equations

$$\frac{Nu (2 + 1.6e^{-As})}{Pr^{0.4} e^{0.0134 Pr} \mu_r^{-0.8}} = 0.172 Re^{(0.0016Pr+0.75)} \quad \text{for smooth wall} \quad (1)$$

$$\frac{Nu (2.05 + 1.62e^{-As})}{Pr^{0.4} e^{0.0134 Pr} \mu_r^{-0.8} (p/e)^{-0.13}} = 0.175 Re^{(0.0016Pr+0.75)} \quad \text{for ribbed wall} \quad (2)$$

5. CONCLUSIONS

The friction factor decreases slightly with the increase of Reynolds number and this can be correlated in line with the other researchers.

The saddle shaped mean velocity profiles in the non-ribbed duct indicate the influence of strong secondary flow on the mean flow field while the hat shaped mean velocity profiles of ribbed duct exhibit the presence of weak secondary flow there. The influence of secondary flow is found to be most prominent near the ribbed wall.

1. The mean velocity profiles across the ribbed wall are found to be asymmetric along the vertical axis due to different wall roughness of the both ribbed and the other three non-ribbed surfaces. Near the rough wall the boundary layer extends more towards the centre than in the non-ribbed wall. This is due to the more increased roughness of the ribbed wall.
2. The temperature distribution clearly shows that the temperature is highest near the side walls and lowest near the central zone. The presence of low velocity associated with strong secondary velocity near the corners of the duct causes this pattern of temperature distribution.
3. The bottom wall temperature of non-ribbed duct is found to increase near the inlet and becomes asymptotic after $X/D_h = 15$ signifying the equilibrium heat flow condition there. But that for the ribbed duct is found to increase up to the end of the duct indicating non-equilibrium heat flow condition.
4. The comparisons between the Nusselt number against Reynolds number are made among the experimental result.
5. The heat absorbed by the flowing air increases with the increase of Reynolds number. The temperature difference of outlet and inlet air is height for lowest p/e ratio i.e. height effective roughness.
6. The Nusselt number of air flowing through the ducts increases with the increase of Reynolds number and corresponding higher values are obtained for lower values of p/e ratios

6. ACKNOWLEDGEMENT

The authors express their thanks to all the staffs of different workshops and laboratories for their co-operation in producing the experimental set up. They also thanks Professor Md. Abul Bashar, Director General, Directorate of Technical Education for allowing Dr.Md.Morad Hossain Mollah to pursue this paper and attained the 7th International Conference on Mechanical Engineering, BUET, Dhaka, Bangladesh

7. REFERENCES

1. Hirota. M., Fujita. H., and Yokosawa. H., "Experimental Study on Convective Heat Transfer for Turbulent Flow in a Square Duct With a Ribbed Rough Wall (Characteristics of Mean Temperature Field)." Journal of Heat Transfer, Vol.116, pp. 332-340, May 1994.
2. Hirota. M., Fujita. H., and Yokosawa, "Forced Convective Heat Transfer in a Turbulent Flow through a Square Duct", Nagoya University, Vol. 40, No.2-Research report, 1980.
3. Han. J. C., and Park. J. S., "Developing Heat Transfer in Rectangular Channels with Rib-Turbulators." International Journal of Heat and Mass Transfer, Vol.31, pp.183-195, 1988.
4. Han. J. C., Park. J. S., and Lie. C. K., "Heat Transfer Enhancement in Channels with Turbulent Promoters." ASME, Journal of Engineering for Gas Turbines and Power, Vol.107,
5. Fujita. H., Hirota. M., and Yokosawa. H., "Experiment of Turbulent Flow in a Square Duct with a Roughened Wall." Memoirs of Faculty of Engineering, Nagoya University, Vol.41, No.2, pp.280-291, 1990b.
6. Fujita. H., Hirota. M., and Yokosawa. H., "Forced

Convection Heat Transfer in a Turbulent Flow Through a Square Duct.” Mem. Faculty of Engineering, Nagoya University, Vol.40, No.2, pp.327-336, 1989.

7. Sparrow. E. M., "Analysis of Laminar Forced Convection Heat Transfer in Entrance Region of Flat Rectangular Ducts," NACA Tech Notes, TN 3331, 1955. pp.628-635, 1985.
8. Melling. A., and Whitelaw. J. H., "Turbulent Flow in a Rectangular Duct", J. Fluid Mech., Vol. 78, part 2, pp. 289-315, 1976.
9. James, D. D., "Forced convection Heat Transfer in ducts of Non-circular section." Ph.D Thesis, Imperial College, University of London, U.K, 1967.
10. Hong. S. W., and A. E. Bergles, "Laminar Flow Heat Transfer in the Entrance Region of Semi-Circular Tubes with Uniform Heat Flux." Internal Journal of Heat and Mass Transfer, Vol.19, pp123-124, 1976.
11. Monohar. R., "Analysis of Laminar Flow Heat Transfer in the Entrance Region of Circular Tubes," Internal Journal of Heat and Mass Transfer, Vol.12, pp.15-22., 1969.
- [12] Ulrichson. D. L., and R. A. Schmitz., "Laminar Flow Heat Transfer in the Entrance Region of Circular Tubes," Internal Journal of Heat and Mass Transfer, Vol.8, pp253-258, 1965.
13. Hwang. C. L., and Fan L. T., "Finite Difference Analysis of Forced Convection Heat Transfer in Entrance Region of a Flat Rectangular Duct." Appl. Sci. Res., Sec. A Vol.13, pp.401-422, 1964.
14. Akhanda. M. A. R., "Enhancement Heat Transfer in Forced Convective Boiling," Ph. D Thesis, University of Manchester Institute of Science and Technology, U.K, 1985.
15. Mollah. M. M. H, "Enhancement of Forced Convection Heat Transfer in Ribbed Roughened Square Ducts." Ph. D Thesis, December-2005, BUET, Dhaka, Bangladesh.

8. NOMENCLAYURE

Symbol	Meaning
A_c	Cross sectional area of the test duct, m^2
A_s	Surface area of the aluminium wall, m^2
B	Half of the side of test duct, $= D/2$, m.
D_h	Equivalent diameter of the duct, m.
C_p	Specific heat of air, $J/kg^\circ C$
δ	Thickness of the aluminium wall. m
G	Mass flux of air flowing in the duct, $kg/m^2 s$
h	Heat transfer coefficient, $W/m^2^\circ C$.
I	Current supplied to the heater , Amp.
L	Length of developing duct, 3 m
Nu	Nusselt number
μ_b	Dynamic viscosity at mean temperature of air, $Kg/m-s$.
μ_w	Dynamic viscosity of air, $kg/m-s$
μ_r	μ_b / μ_w Viscosity ratio.
ρ	Density of air, kg/m^3 .
q_g	Heat energy supplied to the heater, W
q_{cod}	Heat conducted through aluminium wall, W
q_a	Heat energy absorbed by air, W.
q_{conv}	Heat energy convected to air, W.
Pr	Prandtl number
Re	Reynolds number
St	Stanton number
T_{mi}	Average temperature at the inlet, $^\circ C$.
T_{mo}	Ave. temperature at outlet, $^\circ C$.
T_m	Mean temperature of air in duct, $^\circ C$.
T_{wo}	Ave outer surface temp.of Al wall, $^\circ C$.
T_{wi}	Ave inner surface temp.of Al wall, $^\circ C$.
T_c	Temp. at centre line of the duct. $^\circ C$
ΔT	$= (T_{mo} - T_{mi})$ Temp. difference bet ⁿ outlet and inlet of the duct, $^\circ C$.
u_{mi}	Average velocity at the inlet of the test duct. m/s
u_{mo}	Ave. velocity at outlet of test duct. m/s
u_m	Mean velocity of air $= (u_{mi}+u_{mo})/2$.m/s
V	Supply voltage to the heater, Volt.
X, Y, Z	Three axes of the co-ordinate system.